JACS
JOURNAL OF THE AMERICAN CHEMICAL SOCIETY
pubs.acs.org/JACS
Article

N-Heterocyclic Carbenes as Reversible Exciton-Delocalizing Ligands for Photoluminescent Quantum Dots

Dana E. Westmoreland, Rafael López-Arteaga, and Emily A. Weiss*

Cite This: J. Am. Chem. Soc. 2020, 142, 2690−2696
Read Online
ACCESS | Metrics & More | Article Recommendations | Supporting Information

ABSTRACT: Delocalization of excitons within semiconductor quantum dots (QDs) into states at the interface of the inorganic core and organic ligand shell by so-called "exciton-delocalizing ligands (EDLs)" is a promising strategy to enhance coupling of QD excitons with proximate molecules, ions, or other QDs. EDLs thereby enable enhanced rates of charge carrier extraction from, and transport among, QDs and dynamic colorimetric sensing. The application of reported EDLs—which bind to the QDs through thiolates or dithiocarbamates—is however limited by the irreversibility of their binding and their low oxidation potentials, which lead to a high yield of photoluminescence-quenching hole trapping on the EDL. This article describes a new class of EDLs for QDs, 1,3-dimethyl-4,5-disubstituted imidazolylidene N-heterocyclic carbenes (NHCs), where the 4,5-substituents are Me, H, or Cl. Postsynthetic ligand exchange of native oleate capping ligands for NHCs results in a bathochromic shift of the optical band gap of CdSe QDs (R = 1.17 nm) of up to 111 meV while the colloidal stability of the QDs is maintained. This shift is reversible for the MeNHC-capped and HNHC-capped QDs upon protonation of the NHC. The magnitude of exciton delocalization induced by the NHC (after scaling for surface coverage) increases with the increasing acidity of its π system, which depends on the substituent in the 4,5-positions of the imidazolylidene. The NHC-capped QDs maintain photoluminescence quantum yields of up to 4.2 ± 1.8% for shifts of the optical band gap as large as 106 meV.

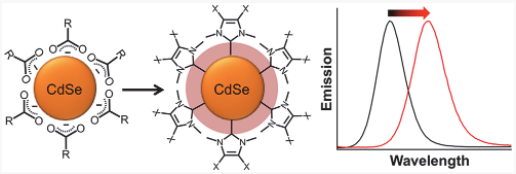

INTRODUCTION

Exciton-delocalizing ligands (EDLs) are a class of molecules that couple quantum-confined electrons within semiconductor nanocrystals to their immediate environments.[1] The orbitals of an EDL with appropriate symmetry and energy mix with conduction or valence band orbitals of the nanocrystal and thereby create new interfacial states into which the nanocrystal's exciton delocalizes. In a series of papers from 2010 to 2013, we introduced phenyldithiocarbamate (PTC) and its para-substituted derivatives as EDLs that decrease the optical band gaps of Cd and Pb chalcogenide quantum dots (QDs) by up to 1 eV without changing the physical structures of their cores.[2−5] Our mechanistic studies on the QD-PTC complexes led to the conclusion that mixing of the σ-character orbitals of PTC and the Cd^{2+} or Pb^{2+} s orbitals of the QD conduction band and mixing of the π-character orbitals of PTC and the chalcogenide p orbitals of the QD valence band relax the quantum confinement of the exciton, primarily the excitonic hole.[3,4,6−9] This "through-bond" mechanism for exciton delocalization was substantiated and elaborated by a series of papers that combine experimental data with density functional theory calculations.[2−4,6,10−12] By an increase in the permeation of the excitonic wave function through the dielectric interface separating the inorganic core and the organic ligand of the colloid, EDLs greatly enhance our ability to, for example, extract the otherwise highly localized excitonic hole from a QD[13−15] (allowing us to achieve the fastest photoreduction of a metal chalcogenide QD recorded and the first photoreduction of the biexcitonic state of a QD),[16] transport excitons through QD films,[17−19] and perform multihole photooxidative reactions with QDs.[16,20]

Much of the physics of the EDL effect is fairly straightforward, but thiolates and PTC derivatives are problematic as EDLs due to their specific chemical structures. First, when it is bound to a metal cation on the QD surface, PTC is very chemically stable, even in air and light, but when it freely diffuses as an acid or salt, PTC degrades within minutes to hours to the corresponding aniline, thiourea, and phenyl isothiocyanate.[6] Although these degradation products do not themselves delocalize the QD exciton, and therefore do not contribute to the observed spectral shift, the degradation makes ligand exchange inefficient and complicates quantification of the yield of ligand exchange. Second, PTC is effectively an irreversible binder; once it is bound to Cd^{2+} or Pb^{2+}, we have not found a way to displace it without also etching the QD core. The tight binding of PTC (and thiolates) makes their mechanism of delocalization difficult to prove because it is not straightforwardly reversible. Finally, and perhaps most

Received: December 17, 2019
Published: January 14, 2020

https://dx.doi.org/10.1021/jacs.9b13605
J. Am. Chem. Soc. 2020, 142, 2690−2696

importantly, PTC and thiolates adsorb in more than one configuration on the QD surface, and some of these binding modes trap the excitonic hole on the ligand rather than delocalizing it through the ligand.[7,21−23] Hole trapping, when it occurs in high yield, efficiently quenches the photoluminescence (PL) of the QD ensemble by limiting electron−hole coupling. Sensing, photovoltaic, and photocatalytic applications of QDs require high photoluminescence quantum yields (QYs), or at least accessible excitonic charge carriers.

Here, we introduce a new class of EDL: 1,3-dimethyl-4,5-disubstituted imidazolylidene N-heterocyclic carbene (NHC) ligands, with hydrogen (H), methyl (Me), or chloride (Cl) substituents (Scheme 1), that address many of the issues with

Scheme 1. Ligand Exchange Procedure[a]

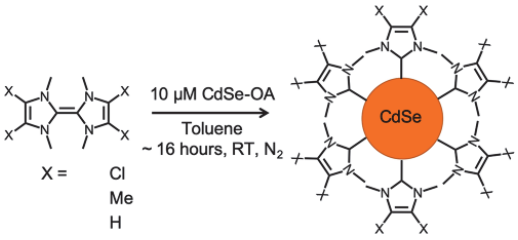

[a]Varying amounts (up to 120 equiv, depending on X) of XNHC dimer were added to 10 μM oleate (OA)-capped CdSe QDs in toluene, and the mixture was stirred at room temperature under an N_2 atmosphere. The cartoon of the NHC-capped QD is not to scale.

dithiocarbamate and thiolate EDLs. We targeted NHCs as EDLs because, much like dithiocarbamates and thiolates, NHCs interact through both s- and p-type orbitals located on the carbene carbon,[24−26] which has the potential to bind to either cadmium[27−29] or selenium[30−32] or both on the QD surface, and because there is literature precedent for NHCs as ligands for metal clusters[33−35] and metal nanoparticles.[36−41] The imidazolylidene NHCs in particular are partially aromatic; thus, modification of substituents at the 4,5-positions affects their π acidity and should affect the degree of exciton delocalization enabled by the molecule.[42] We find that all three NHC derivatives studied in this work delocalize the QD exciton; as expected for an EDL, the magnitude of the apparent increase in excitonic radius (ΔR) per bound NHC ligand depends on the substituent. Unlike PTC-capped QDs, (i) HNHC- and MeNHC-capped QDs maintain PL QYs of 0.6 ± 0.1% and 4.8 ± 1.7%, respectively, at an optical shift of 92 meV and (ii) the exciton delocalization induced by HNHC and MeNHC is *reversible* upon protonation and subsequent desorption of the NHC.

The spectral shift induced by ClNHC is not reversible, and its adsorption does not preserve the PL of the QDs (for reasons explained in the text). We nonetheless include it in our data set, because comparison of its EDL effect to those of HNHC and MeNHC allows us to correlate the EDL effect of an NHC ligand with its π acidity, a correlation that is consistent with our proposed mechanism for exciton delocalization by dithiocarbamates and thiolates.

RESULTS AND DISCUSSION

We synthesized CdSe QDs with an average radius of 1.17 nm and oleate capping ligands according to a previously published procedure[43] and purified the oleate-capped QDs by sequential precipitation with acetone followed by methanol (see the Supporting Information for details). We synthesized the MeNHC and HNHC precursor salts according to a patented procedure[44] and the ClNHC precursor salt according to a published procedure (see the Supporting Information for details).[45] Under an N_2 atmosphere, we deprotonated the 1,3-dimethyl-4,5-disubstituted imidazolium salts with a minimum of 1.2 equiv of sodium hydride and 3 mol % cesium carbonate in anhydrous THF.[46] After the reaction was allowed to proceed for at least 4 h for the ClNHC and HNHC derivatives or between 13 and 18 h for the MeNHC derivative, we filtered the solution through Celite and washed with additional THF. The resulting NHC derivatives exist predominantly as dimers in THF (see Figure S1 of the Supporting Information).[47,48] All optical measurements of the NHC-capped QDs were performed using air-free cuvettes unless otherwise indicated, and all NMR measurements were performed using J. Young tubes to ensure an air- and water-free environment.

Scheme 1 depicts the procedure that we used to exchange the native oleate ligands on the QDs for each type of NHC ligand. Under an N_2 atmosphere, we added an aliquot of the prescribed concentration of the XNHC dimer in a THF stock solution to an anhydrous toluene solution of 10 μM CdSe QDs and allowed the ligand exchange to proceed for 12−18 h (overnight) at room temperature. Upon addition of the NHC derivatives, a population of freely diffusing oleate (or oleic acid) appeared in the ^{1}H NMR spectra of the samples; some residual QD-bound oleate remained (see Figure S2 of the Supporting Information). It appears that MeNHC and ClNHC react with the double bond of oleate, which prevented us from accurately quantifying the remaining coverage of oleate ligands (see Table S1 of the Supporting Information). This reaction, which we have not characterized, does not appear to occur with HNHC, and we can determine that each added HNHC displaces 2.3 ± 0.3 oleate ligands from the QD surface (see Table S2 of the Supporting Information). We did not wash out free oleate or unbound NHC dimers prior to characterization of the NHC-capped QDs to avoid stripping bound NHC ligands from the QD surface during washing. The resulting MeNHC-, HNHC-, and ClNHC-capped QDs are colloidally stable in toluene under an N_2 atmosphere for at least 2 days (see Figure S3 of the Supporting Information).

Consistent with the effects of dithiocarbamate[2−4] and thiolate[7,22,23] EDLs, ligand exchange from oleate to XNHC bathochromically shifts the absorbance spectrum of the QD ensemble; the shift corresponds to a decrease in the energy of the QD's first excitonic state by an amount (ΔE) that depends on (i) the coverage of XNHC and (ii) the substituent, X. Figure 1A shows the maximum achievable bathochromic shift of the ground-state absorbance spectrum of 1.2 μM CdSe QDs (physical radius of 1.17 nm) while maintaining colloidal stability, upon treatment of oleate-capped QDs (black) with MeNHC (red, ΔE = 115 meV), ClNHC (green, ΔE = 48 meV), or HNHC (blue, ΔE = 111 meV). The emission spectra for the data shown in Figure 1A show a corresponding bathochromic shift, except for the ClNHC-capped QDs, which are nonemissive (see Figure S4 of the Supporting Information). At >80 added equiv, the MeNHC-capped QDs precipitated from solution (see Figure S5A of the Supporting Information), as has been seen with Pd nanoparticles capped with NHCs with short-chain aliphatic groups in the 4- and 5-positions of the imidazolylidene.[49] For the ClNHC-capped

https://dx.doi.org/10.1021/jacs.9b13605
J. Am. Chem. Soc. 2020, 142, 2690−2696

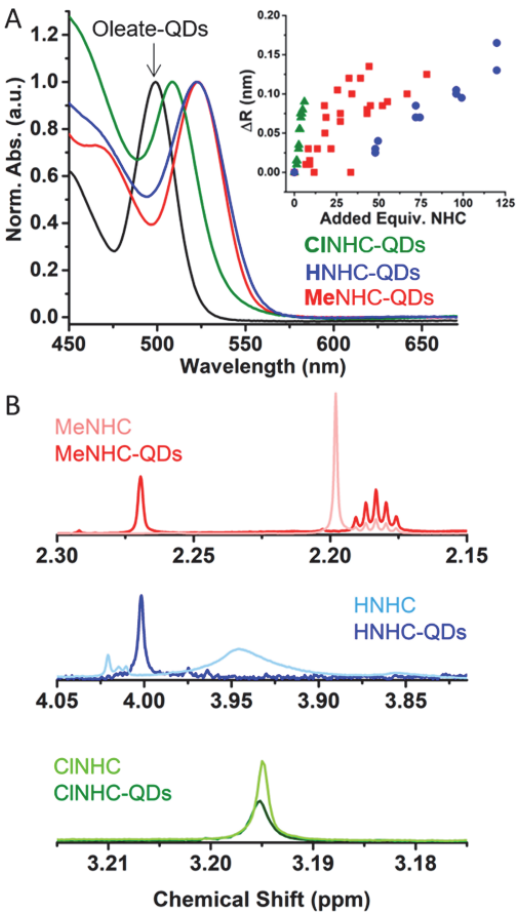

Figure 1. (A) Ground-state absorbance spectra of 10 μM oleate-capped CdSe QDs in toluene (black) and of those same QDs after treatment with 6 equiv of ClNHC (green), 78 equiv of MeNHC (red), or 120 equivof HNHC (blue). All spectra are normalized to the first absorption maximum. We occasionally observed minor shifts in absorbance baseline due to a fraction of the QDs aggregating during ligand exchange; the Supporting Information describes how we manually subtract those baselines from the spectra before analyzing any spectral shift. Inset: a plot of the apparent change in the average excitonic radius of the QD ensemble, "ΔR", vs added equivalents of each NHC derivative. The data sets include measurements on at least three separately prepared sets of samples for each NHC derivative. (B) ^{1}H NMR spectra of each NHC derivative in d_8-toluene with and without 6.6 μM CdSe QDs (45 equiv of MeNHC/QD), 7.6 μM QDs (77 equiv of HNHC/QD), or 6.9 μM QDs (2 equiv of ClNHC/QD). The quintet at 2.18 ppm (top) is a satellite peak of residual THF. The peaks at 4.02 ppm (middle) are due to impurities introduced during the deprotonation of the HNHC.

QDs, precipitation occurred at >6 equiv added, while for the HNHC-capped QDs, precipitation did not occur until >120 equiv were added (see Figure S5B,C of the Supporting Information).

We translate these ΔE values into "ΔR", defined as the apparent increase in average excitonic radius of the QDs within the ensemble due to the EDL effect. The ΔR parameter is a convenient means of comparing EDL effects among different QD materials, ligand structures, and coverages. Figure 1A (inset) is a plot of ΔR versus added equivalents of each NHC derivative over the linear region of this plot (i.e., before colloidal stability is compromised; see Figure S5 of the Supporting Information). HNHC produces the largest ΔR without the loss of the QD colloidal stability, 0.165 nm; this value is on the order of the maximum ΔR value (0.175 nm) achieved by treating CdSe QDs with unsubstituted PTC.[3] Addition of 50 equiv of the protonated forms of MeNHC or ClNHC, or 400 equiv of the protonated form of HNHC, which should *not* bind to the QD surface, results in no shift of the absorbance or emission of the QDs (see Figure S6 of the Supporting Information).

Figure 1B shows portions of the ^{1}H NMR spectra of each freely diffusing NHC in d_8-toluene and the same compound upon addition of 7−8 μM QDs. We scale the NMR spectra with and without QDs to correct for dilution (see the Supporting Information for details). We know that the peaks in these six spectra are attributable to the dimer of each XNHC from ^{13}C NMR (see Figure S7 of the Supporting Information), because their peak positions are not consistent with those previously reported for the monomeric species.[46] The top spectra show the MeNHC dimer peak for the backbone methyl groups at 2.26 ppm with QDs and at 2.20 ppm without QDs. In d_8-toluene, the wingtip protons are buried beneath residual THF at 3.54 ppm (see Figure S8 of the Supporting Information). The middle spectrum shows the HNHC dimer peak for the wingtip protons at 4.00 ppm with QDs and at 3.95 ppm (and broadened) without QDs. The broadening of the peak for the freely diffusing HNHC dimer is due to the low solubility of this molecule in d_8-toluene; the QDs, and associated oleate ligands, help to bring the HNHC into solution. The bottom spectrum in Figure 1B shows the ClNHC dimer peak at 3.20 ppm with QDs and 3.19 ppm without QDs. A downfield shift and slight broadening of the peak upon addition of QDs is consistent with dynamic exchange of the molecule (through the monomer species) on and off the QD surface on a time scale faster than that of the NMR experiment.[49−52] We suspect, but have not proven, that the difference in chemical shift between the resonances for the bound monomer and freely diffusing dimer of ClNHC is very small because this shift has a large contribution from NHC−NHC interactions on the QD surface, and we added only 2 equiv/QD of ClNHC (as opposed to the tens of equivalents of MeNHC and HNHC) in this experiment.

The inset of Figure 1A demonstrates that ΔR increases with increasing added XNHC but does not account for the different binding equilibria of the various XNHCs and therefore does not allow us to connect the molecular structure of each XNHC to the magnitude of its EDL effect. To probe the mechanism of exciton delocalization by NHCs, we need the value of ΔR per *bound* XNHC, which we denote ΔR_b. NMR is not useful for quantifying the number of XNHCs bound because excess MeNHC and ClNHC dimer appear to react with oleate (see Table S1 of the Supporting Information) and because the freely diffusing HNHC dimer is only marginally soluble in d_8-toluene. We instead determine the value of ΔR_b by monitoring the position of the first excitonic peak of the QDs upon addition of various concentrations of *p*-toluenesulfonic acid (TsOH), which protonates XNHC molecules on the QD surface, induces their desorption, and causes the QD band gap

https://dx.doi.org/10.1021/jacs.9b13605
J. Am. Chem. Soc. 2020, 142, 2690−2696

to shift back toward its original value (that corresponding to oleate-coated QDs).

This experiment relies on the reversibility of the EDL effect of the XNHCs; the lack of reversibility of the optical shift of dithiocarbamate-treated QDs was a notable weakness of this class of EDL ligands. Figure 2A,B shows that the optical shift induced by 15 equiv of MeNHC is completely reversible upon addition of 30 μL of 40 mM TsOH solution (50 equiv of TsOH/QD) in acetonitrile to 6 μM QDs and that the shift induced by addition of 64 equiv of HNHC is completely reversible upon addition of 100 μL of 40 mM TsOH solution (122 equiv of TsOH/QD). The optical band gap of the QDs returns to its value before NHC treatment; NMR evidence that this reversion is due to protonation of the NHC off the surface of the QD is given in Figures S9 and S10 of the Supporting Information. The number of equivalents of MeNHC and HNHC we added in this experiment was limited by the amount of TsOH the QDs would tolerate before their emission was quenched, not the degree to which their EDL effect is reversible (see Figure S11 of the Supporting Information). The shift in the QDs' optical band gap by ClNHC is not reversible upon addition of TsOH (Figure 2C), presumably due to stripping of both the ClNHC and residual oleate from the QD surface, which results in aggregation and precipitation of the QDs after the addition of 36 equiv of TsOH per QD (see Figure S12 of the Supporting Information).

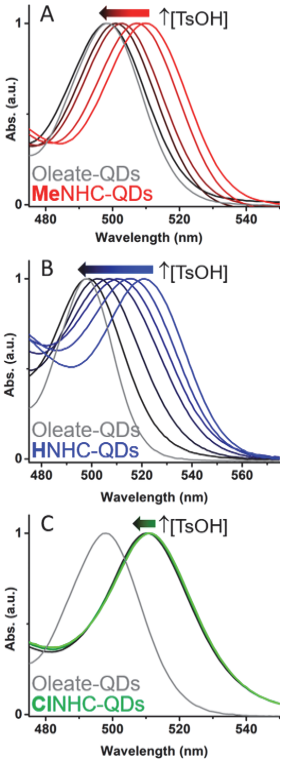

Figure 2. Normalized and baseline-subtracted absorbance spectra for 10 μM CdSe QDs treated with 15 equiv of MeNHC (A), 64 equiv of HNHC (B), or 4 equiv of ClNHC (C) upon addition of various equivalents per QD (up to 50 equiv for MeNHC-capped QDs, 122 equiv for HNHC-capped QDs, and 36 equiv for ClNHC-capped QDs) of 40 mM *p*-toluenesulfonic acid (TsOH) in acetonitrile solution. The ClNHC-capped QDs precipitate upon addition of TsOH, as described in the text.

To estimate the average number of XNHC ligands that desorb from each QD for each added amount of TsOH—and therefore determine the number of bound XNHC ligands that correspond to a certain shift in the absorption spectrum, ΔE—we measure the number of freely diffusing XNHC molecules that are protonated upon addition of various equivalents of TsOH (in the absence of QDs). We measure this number through the disappearance of the dimer signal in the NMR spectra in d_8-toluene of each XNHC (see Figure S13 of the Supporting Information), since the protonated NHCs with *p*-toluenesulfonate counterions are insoluble in toluene. We then assume that the pK_a value of the QD-associated NHC derivatives is similar to that of the free NHC dimers in solution, since the species are in equilibrium, such that we can convert "equivalents of TsOH added" to an XNHC-capped QD sample to "equivalents of XNHC desorbed" for that sample. We then determine the energy by which the band gap of the QDs increases (decreases) upon desorption (adsorption) of a given number of XNHC ligands and plot ΔR vs equivalents of MeNHC and HNHC bound to the QD surface in Figure 3. The slope of this line is ΔR_b, the value of ΔR per *bound* XNHC.

We cannot do such an analysis for ClNHC because its binding is not reversible under conditions where the QDs remain colloidally stable, due to the initial displacement of the

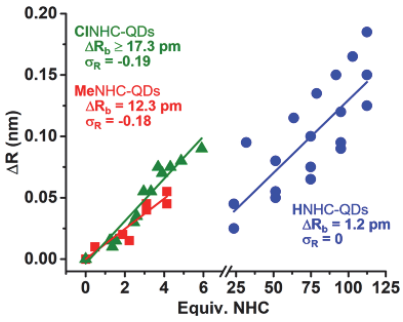

Figure 3. Change in the apparent excitonic radius of the QDs, "ΔR", versus the number of equivalents of MeNHC (red squares), ClNHC (green triangles), and HNHC (blue circles) per QD. For MeNHC and HNHC, the *x* axis is "Equivalents of NHC *bound* per QD", as determined from the TsOH titration described in the text. For ClNHC, the *x* axis is "Equivalents of NHC *added* per QD". The data are fit with lines with slopes of ΔR_b, defined as ΔR per equivalent of bound NHC (or added, in the case of ClNHC). Since the equivalents of ClNHC added per QD are upper bounds for ClNHC bound per QD, the value of ΔR_b for ClNHC listed in the caption is a lower limit for the actual value of ΔR_b. We can therefore conclude that ΔR_b(ClNHC) $\gtrsim$ ΔR_b(MeNHC) > ΔR_b(HNHC). "σ_R" is the Hammett resonance parameter for the correspondingly substituted benzoic acid: $|\sigma_R|$(ClNHC) $\gtrsim$ $|\sigma_R|$(MeNHC) > $|\sigma_R|$(HNHC). The data sets include measurements on at least three separately prepared sets of samples for each NHC derivative.

https://dx.doi.org/10.1021/jacs.9b13605
J. Am. Chem. Soc. 2020, 142, 2690−2696

majority of the oleate ligands during the ligand exchange with ClNHC (see Figure S2 of the Supporting Information). We therefore plot in Figure 3 ΔR vs equivalents of ClNHC added. The value of ΔR_b extracted from this plot is a lower limit for the actual ΔR_b value for this ligand.

From Figure 3, we conclude that (i) ΔR_b for XNHC depends on X, a result consistent with the dependence of ΔR_b of para-substituted phenyldithiocarbamate ligands on their substituents,[4] and (ii) ΔR_b(ClNHC) $\gtrsim$ ΔR_b(MeNHC) > ΔR_b(HNHC). NHC ligands are strong σ donors but may also show significant π acidity depending on the nature of the backbone substituents.[53] Density functional theory calculations of the orbital energies of cadmium complexes of each XNHC suggest that exciton delocalization could occur through ground-state electron transfer from the QD valence band to the π-type LUMO+1 of the Cd^{2+}-bound XNHC (see Figures S14 and S15 of the Supporting Information). Such a mechanism would imply that the strongest π-acceptor NHC of the series should also be the most strongly exciton delocalizing ligand (and have the largest ΔR_b). One measure of π acidity is the Hammett resonance parameter, σ_R, for a given substituent. The values of σ_R for the three substituents in our study are given in the caption of Figure 3: $|\sigma_R|$(Cl) $\gtrsim$ $|\sigma_R|$(Me) > $|\sigma_R|$(H).[54,55] This trend explains our result: ΔR_b(ClNHC) $\gtrsim$ ΔR_b(MeNHC) > ΔR_b(HNHC). Additionally, ^{77}Se NMR studies of Se−XNHC adducts, where the NHC is a H- or Cl-disubstituted imidazolylidene with dipp wingtip groups, support our conclusion that ClNHC is a stronger π-donor than HNHC.[30] There has been no report comparing the π acidities of HNHC, ClNHC, and MeNHC; methods involving changes in the CO stretching frequency trans to an NHC ligand for a metal center do not isolate the influence of the π acidity of the NHC ligand on this frequency.

The results in Figure 3 are consistent with our picture of the interfacial electronic structure of phenyldithiocarbamate-capped QDs,[4] in that the σ interaction between the EDL and a metal cation on the QD surface allows for adsorption of the EDL, while mixing of orbitals within the valence band of the QD and a π-type orbital or orbitals on the ligand mediates the ground state charge transfer-type interaction necessary for exciton delocalization. The degree of this charge transfer, dictated by the electron-accepting ability of those ligand π-type orbitals, determines the magnitude of the EDL effect and the degree to which the optical spectrum of the QD shifts.

Unlike with PTC ligands, we detect PL of the NHC-capped QDs without the addition of a cadmium salt, which, in the PTC case, was needed to precipitate excess PTC that would otherwise bind as a hole trapping ligand.[21] Figure 4 shows the photoluminescence quantum yield (PL QY) of the QDs as a function of increasing equivalents of each XNHC bound to the QD surface, plotted as the ΔR value for each sample.[56] We observe an initial increase in the PL QY upon the addition of MeNHC and HNHC, followed by a decrease. Addition of ClNHC results in quenching of the PL QY even upon addition of <1 equiv. We suspect this quenching is due to decreased surface passivation upon oleate desorption and subsequent aggregation of these particles (see Figures S2 and S5B of the Supporting Information).

CONCLUSIONS

In summary, we demonstrate the use of 1,3-dimethyl-4,5-disubstituted imidazolylidene XNHC (X = H, Me, Cl) ligands as exciton-delocalizing ligands (EDLs) for CdSe QDs; the magnitude of the delocalization effect, which appears as a bathochromic shift of the absorption and emission spectra of the QDs of up to 0.111 eV, increases with the π acidity of the XNHC ligand. This trend is consistent with the mechanism proposed for exciton delocalization by phenyldithiocarbamate and thiolate EDLs in that the σ interaction between the ligand and a surface Cd^{2+} enables binding of the NHC ligands to the surface, but the mixing of π orbitals on the carbene carbon with the QD valence band enables the exciton delocalization to occur.

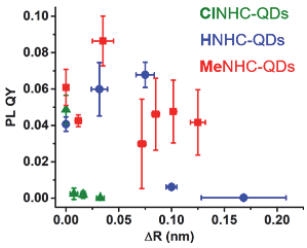

Figure 4. Fractional photoluminescence quantum yields (PL QY) of a set of samples of QDs in toluene, relative to that of quinine sulfate in 0.1 M aqueous H_2SO_4, after treatment with various concentrations of MeNHC, ClNHC, or HNHC, vs the values of ΔR for those samples. The excitation wavelength used to acquire the emission spectra, which are given in Figure S16 of the Supporting Information, is 450 nm.

This work broadens the scope of colloidal nanoparticle applications of NHCs, which until now has been limited to NHC-capped metal nanoparticles[36−41] and clusters[33−35] and the synthetic precursors of coinage-metal chalcogenide QDs.[57] It also broadens the scope of EDLs beyond those containing thiolate binding groups and simultaneously overcomes two of the major limitations of sulfur-containing EDLs: the lack of reversibility of exciton delocalization (due to lack of reversible binding to the QD surface) and the of lack of PL without the addition of excess cadmium salts to the solution following ligand exchange. In contrast, titration of MeNHC- and HNHC-capped QDs with TsOH results in full reversibility of the bathochromic shift induced upon ligand exchange with these NHC derivatives, which we attribute to protonation and subsequent desorption of the MeNHC and HNHC ligands from the QD surface. The NHC-capped QDs maintain photoluminescence quantum yields of up to 4.2 ± 1.8% for shifts of the optical band gap as large as 106 meV. The conservation of PL of the QDs at coverages of MeNHC and HNHC that display a change in PL peak position which is 87% of the PL line width suggests that NHC-capped QDs may be useful as colorometric sensors. The lack of hole trapping by these EDLs also suggests that they may greatly enhance the rates of direct charge carrier extraction to NHC-linked molecular acceptors in, for instance, photocatalytic applications.

ASSOCIATED CONTENT

Supporting Information

The Supporting Information is available free of charge at https://pubs.acs.org/doi/10.1021/jacs.9b13605.

Details of QD and XNHC syntheses, ligand exchange procedure, ^{1}H NMR experiments, and ground state spectroscopy experiments, including Figures S1−S16 and Tables S1 and S2 (PDF)

https://dx.doi.org/10.1021/jacs.9b13605
J. Am. Chem. Soc. 2020, 142, 2690−2696

AUTHOR INFORMATION

Corresponding Author

Emily A. Weiss − *Department of Chemistry, Northwestern University, Evanston, Illinois 60208-3113, United States;* orcid.org/0000-0001-5834-463X; Email: e-weiss@northwestern.edu

Authors

Dana E. Westmoreland − *Department of Chemistry, Northwestern University, Evanston, Illinois 60208-3113, United States*

Rafael López-Arteaga − *Department of Chemistry, Northwestern University, Evanston, Illinois 60208-3113, United States*

Complete contact information is available at: https://pubs.acs.org/10.1021/jacs.9b13605

Notes

The authors declare no competing financial interest.

ACKNOWLEDGMENTS

This work was supported by the National Science Foundation (grant no. CHE-1664184) and the National Institutes of Health (grant no. R21GM127919). We utilized instrumentation in the IMSERC facility at Northwestern University, which has received support from the Soft and Hybrid Nanotechnology Experimental (SHyNE) Resource (NSF ECCS-1542205), the NIH (1S10OD012016-01/1S10RR019071-01A1), the state of Illinois, and the International Institute for Nanotechnology (IIN). We kindly thank Mark Maskeri, Dan Laorenza, Dr. Agnes Thorarinsdottir, and Dr. Andrea D'Aquino for helpful discussions.

REFERENCES

(1) Frederick, M. T.; Amin, V. A.; Weiss, E. A. Optical Properties of Strongly Coupled Quantum Dot−Ligand Systems. *J. Phys. Chem. Lett.* **2013**, *4* (4), 634−640.

(2) Frederick, M. T.; Weiss, E. A. Relaxation of Exciton Confinement in CdSe Quantum Dots by Modification with a Conjugated Dithiocarbamate Ligand. *ACS Nano* **2010**, *4* (6), 3195−3200.

(3) Frederick, M. T.; Amin, V. A.; Cass, L. C.; Weiss, E. A. A Molecule to Detect and Perturb the Confinement of Charge Carriers in Quantum Dots. *Nano Lett.* **2011**, *11* (12), 5455−5460.

(4) Frederick, M. T.; Amin, V. A.; Swenson, N. K.; Ho, A. Y.; Weiss, E. A. Control of Exciton Confinement in Quantum Dot−Organic Complexes through Energetic Alignment of Interfacial Orbitals. *Nano Lett.* **2013**, *13* (1), 287−292.

(5) Teunis, M. B.; Dolai, S.; Sardar, R. Effects of Surface-Passivating Ligands and Ultrasmall CdSe Nanocrystal Size on the Delocalization of Exciton Confinement. *Langmuir* **2014**, *30* (26), 7851−7858.

(6) Harris, R. D.; Amin, V. A.; Lau, B.; Weiss, E. A. Role of Interligand Coupling in Determining the Interfacial Electronic Structure of Colloidal CdS Quantum Dots. *ACS Nano* **2016**, *10* (1), 1395−1403.

(7) Amin, V. A.; Aruda, K. O.; Lau, B.; Rasmussen, A. M.; Edme, K.; Weiss, E. A. Dependence of the Band Gap of CdSe Quantum Dots on the Surface Coverage and Binding Mode of an Exciton-Delocalizing Ligand, Methylthiophenolate. *J. Phys. Chem. C* **2015**, *119* (33), 19423−19429.

(8) Aruda, K. O.; Amin, V. A.; Thompson, C. M.; Lau, B.; Nepomnyashchii, A. B.; Weiss, E. A. Description of the Adsorption and Exciton Delocalizing Properties of p-Substituted Thiophenols on CdSe Quantum Dots. *Langmuir* **2016**, *32* (14), 3354−3364.

(9) Giansante, C. Surface Chemistry Control of Colloidal Quantum Dot Band Gap. *J. Phys. Chem. C* **2018**, *122* (31), 18110−18116.

(10) Li, W.; Lu, T.-F.; Ren, W.; Deng, L.; Zhang, X.; Wang, L.; Tang, J.; Kuznetsov, A. E. Influence of an exciton-delocalizing ligand on the structural, electronic, and spectral features of the Cd33S33 quantum dot: insights from computational studies. *J. Mater. Chem. C* **2018**, *6* (32), 8751−8761.

(11) Azpiroz, J. M.; De Angelis, F. Ligand Induced Spectral Changes in CdSe Quantum Dots. *ACS Appl. Mater. Interfaces* **2015**, *7* (35), 19736−19745.

(12) Giansante, C.; Infante, I.; Fabiano, E.; Grisorio, R.; Suranna, G. P.; Gigli, G. Darker-than-Black" PbS Quantum Dots: Enhancing Optical Absorption of Colloidal Semiconductor Nanocrystals via Short Conjugated Ligands. *J. Am. Chem. Soc.* **2015**, *137* (5), 1875−1886.

(13) Lian, S.; Weinberg, D. J.; Harris, R. D.; Kodaimati, M. S.; Weiss, E. A. SubpicosecondPhotoinduced Hole Transfer from a CdS Quantum Dot to a Molecular Acceptor Bound Through an Exciton-Delocalizing Ligand. *ACS Nano* **2016**, *10* (6), 6372−6382.

(14) Lee, J. R.; Li, W.; Cowan, A. J.; Jäckel, F. Hydrophilic, Hole-Delocalizing Ligand Shell to Promote Charge Transfer from Colloidal CdSe Quantum Dots in Water. *J. Phys. Chem. C* **2017**, *121* (28), 15160−15168.

(15) Xie, Y.; Teunis, M. B.; Pandit, B.; Sardar, R.; Liu, J. Molecule-like CdSe Nanoclusters Passivated with Strongly Interacting Ligands: Energy Level Alignment and Photoinduced Ultrafast Charge Transfer Processes. *J. Phys. Chem. C* **2015**, *119* (5), 2813−2821.

(16) Lian, S.; Christensen, J. A.; Kodaimati, M. S.; Rogers, C. R.; Wasielewski, M. R.; Weiss, E. A. Oxidation of a Molecule by the Biexcitonic State of a CdS Quantum Dot. *J. Phys. Chem. C* **2019**, *123* (10), 5923−5930.

(17) Azzaro, M. S.; Le, A. K.; Wang, H.; Roberts, S. T. Ligand-Enhanced Energy Transport in Nanocrystal Solids Viewed with Two-Dimensional Electronic Spectroscopy. *J. Phys. Chem. Lett.* **2019**, *10* (18), 5602−5608.

(18) Azzaro, M. S.; Dodin, A.; Zhang, D. Y.; Willard, A. P.; Roberts, S. T. Exciton-Delocalizing Ligands Can Speed Up Energy Migration in Nanocrystal Solids. *Nano Lett.* **2018**, *18* (5), 3259−3270.

(19) Zotti, G.; Vercelli, B.; Berlin, A.; Virgili, T. Multilayers of CdSe Nanocrystals and Bis(dithiocarbamate) Linkers Displaying Record Photoconduction. *J. Phys. Chem. C* **2012**, *116* (49), 25689−25693.

(20) Wolff, C. M.; Frischmann, P. D.; Schulze, M.; Bohn, B. J.; Wein, R.; Livadas, P.; Carlson, M. T.; Jäckel, F.; Feldmann, J.; Würthner, F.; Stolarczyk, J. K. All-in-one visible-light-driven water splitting by combining nanoparticulate and molecular co-catalysts on CdS nanorods. *Nat. Energy* **2018**, *3* (10), 862−869.

(21) Jin, S.; Harris, R. D.; Lau, B.; Aruda, K. O.; Amin, V. A.; Weiss, E. A. Enhanced Rate of Radiative Decay in CdSe Quantum Dots upon Adsorption of an Exciton-Delocalizing Ligand. *Nano Lett.* **2014**, *14* (9), 5323−5328.

(22) Buckley, J. J.; Couderc, E.; Greaney, M. J.; Munteanu, J.; Riche, C. T.; Bradforth, S. E.; Brutchey, R. L. Chalcogenol Ligand Toolbox for CdSe Nanocrystals and Their Influence on Exciton Relaxation Pathways. *ACS Nano* **2014**, *8* (3), 2512−2521.

(23) Liang, Y.; Thorne, J. E.; Parkinson, B. A. Controlling the Electronic Coupling between CdSe Quantum Dots and Thiol Capping Ligands via pH and Ligand Selection. *Langmuir* **2012**, *28* (30), 11072−11077.

(24) Nelson, D. J.; Nolan, S. P. Quantifying and understanding the electronic properties of N-heterocyclic carbenes. *Chem. Soc. Rev.* **2013**, *42* (16), 6723−6753.

(25) Huynh, H. V. Electronic Properties of N-Heterocyclic Carbenes and Their Experimental Determination. *Chem. Rev.* **2018**, *118* (19), 9457−9492.

(26) Hopkinson, M. N.; Richter, C.; Schedler, M.; Glorius, F. An overview of N-heterocyclic carbenes. *Nature* **2014**, *510* (7506), 485−496.

(27) Arduengo, A. J.; Goerlicha, J. R.; Davidson, F.; Marshall, W. J. Carbene Adducts of Dimethylcadmium. *Z. Naturforsch., B: J. Chem. Sci.* **1999**, *54*, 1350.
(28) Roy, M. M. D.; Ferguson, M. J.; McDonald, R.; Rivard, E. Investigation of N-Heterocyclic Carbene-Supported Group 12 Triflates as Pre-catalysts for Hydrosilylation/Borylation. *Chem. - Eur. J.* **2016**, *22* (50), 18236−18246.
(29) Bellan, E. V.; Poddel'sky, A. I.; Protasenko, N. A.; Cherkasov, A. V.; Bogomyakov, A. S.; Cherkasov, V. K.; Abakumov, G. A. Bis-o-semiquinonato cadmium(II) complexes with o-quinonato and N-heterocyclic carbene neutral ligands. *Inorg. Chem. Commun.* **2014**, *50*, 1−3.
(30) Verlinden, K.; Buhl, H.; Frank, W.; Ganter, C. Determining the Ligand Properties of N-Heterocyclic Carbenes from 77Se NMR Parameters. *Eur. J. Inorg. Chem.* **2015**, *2015* (14), 2416−2425.
(31) Buhl, H.; Verlinden, K.; Ganter, C.; Novaković, S. B.; Bogdanović, G. A. Electrostatic Properties of N-Heterocyclic Carbenes Obtained by Experimental Charge-Density Analysis of Two Selenium Adducts. *Eur. J. Inorg. Chem.* **2016**, *2016* (21), 3389−3395.
(32) Liske, A.; Verlinden, K.; Buhl, H.; Schaper, K.; Ganter, C. Determining the π-Acceptor Properties of N-Heterocyclic Carbenes by Measuring the 77Se NMR Chemical Shifts of Their Selenium Adducts. *Organometallics* **2013**, *32* (19), 5269−5272.
(33) Smith, C. A.; Narouz, M. R.; Lummis, P. A.; Singh, I.; Nazemi, A.; Li, C.-H.; Crudden, C. M. N-Heterocyclic Carbenes in Materials Chemistry. *Chem. Rev.* **2019**, *119* (8), 4986−5056.
(34) Narouz, M. R.; Osten, K. M.; Unsworth, P. J.; Man, R. W. Y.; Salorinne, K.; Takano, S.; Tomihara, R.; Kaappa, S.; Malola, S.; Dinh, C.-T.; Padmos, J. D.; Ayoo, K.; Garrett, P. J.; Nambo, M.; Horton, J. H.; Sargent, E. H.; Häkkinen, H.; Tsukuda, T.; Crudden, C. M. N-heterocyclic carbene-functionalized magic-number gold nanoclusters. *Nat. Chem.* **2019**, *11* (5), 419−425.
(35) Narouz, M. R.; Takano, S.; Lummis, P. A.; Levchenko, T. I.; Nazemi, A.; Kaappa, S.; Malola, S.; Yousefalizadeh, G.; Calhoun, L. A.; Stamplecoskie, K. G.; Häkkinen, H.; Tsukuda, T.; Crudden, C. M. Robust, Highly Luminescent Au13 Superatoms Protected by N-Heterocyclic Carbenes. *J. Am. Chem. Soc.* **2019**, *141* (38), 14997−15002.
(36) Tegeder, P.; Freitag, M.; Chepiga, K. M.; Muratsugu, S.; Möller, N.; Lamping, S.; Tada, M.; Glorius, F.; Ravoo, B. J. N-Heterocyclic Carbene-Modified Au−Pd Alloy Nanoparticles and Their Application as Biomimetic and Heterogeneous Catalysts. *Chem. - Eur. J.* **2018**, *24* (70), 18682−18688.
(37) Martínez-Prieto, L. M.; Rakers, L.; López-Vinasco, A. M.; Cano, I.; Coppel, Y.; Philippot, K.; Glorius, F.; Chaudret, B.; van Leeuwen, P. W. N. M. Soluble Platinum Nanoparticles Ligated by Long-Chain N-Heterocyclic Carbenes as Catalysts. *Chem. - Eur. J.* **2017**, *23* (52), 12779−12786.
(38) Rakers, L.; Martínez-Prieto, L. M.; López-Vinasco, A. M.; Philippot, K.; van Leeuwen, P. W. N. M.; Chaudret, B.; Glorius, F. Ruthenium nanoparticles ligated by cholesterol-derived NHCs and their application in the hydrogenation of arenes. *Chem. Commun.* **2018**, *54* (51), 7070−7073.
(39) Möller, N.; Rühling, A.; Lamping, S.; Hellwig, T.; Fallnich, C.; Ravoo, B. J.; Glorius, F. Stabilization of High Oxidation State Upconversion Nanoparticles by N-Heterocyclic Carbenes. *Angew. Chem., Int. Ed.* **2017**, *56* (15), 4356−4360.
(40) Ernst, J. B.; Muratsugu, S.; Wang, F.; Tada, M.; Glorius, F. Tunable Heterogeneous Catalysis: N-Heterocyclic Carbenes as Ligands for Supported Heterogeneous Ru/K-Al2O3 Catalysts To Tune Reactivity and Selectivity. *J. Am. Chem. Soc.* **2016**, *138* (34), 10718−10721.
(41) Ernst, J. B.; Schwermann, C.; Yokota, G.-i.; Tada, M.; Muratsugu, S.; Doltsinis, N. L.; Glorius, F. Molecular Adsorbates Switch on Heterogeneous Catalysis: Induction of Reactivity by N-Heterocyclic Carbenes. *J. Am. Chem. Soc.* **2017**, *139* (27), 9144−9147.
(42) Heinemann, C.; Müller, T.; Apeloig, Y.; Schwarz, H. On the Question of Stability, Conjugation, and "Aromaticity" in Imidazol-2-ylidenes and Their Silicon Analogs. *J. Am. Chem. Soc.* **1996**, *118* (8), 2023−2038.
(43) Flamee, S.; Cirillo, M.; Abe, S.; De Nolf, K.; Gomes, R.; Aubert, T.; Hens, Z. Fast, High Yield, and High Solid Loading Synthesis of Metal Selenide Nanocrystals. *Chem. Mater.* **2013**, *25* (12), 2476−2483.
(44) Ren, R. X.; Koch, V. R. One-step process for the preparation of halide-free hydrophobic salts. U.S. Patent 20040225131A1, Nov 11, 2004.
(45) Solovyev, A.; Ueng, S.-H.; Monot, J.; Fensterbank, L.; Malacria, M.; Lacôte, E.; Curran, D. P. Estimated Rate Constants for Hydrogen Abstraction from N-Heterocyclic Carbene-Borane Complexes by an Alkyl Radical. *Org. Lett.* **2010**, *12* (13), 2998−3001.
(46) Arduengo, A. J.; Dias, H. V. R.; Harlow, R. L.; Kline, M. Electronic stabilization of nucleophilic carbenes. *J. Am. Chem. Soc.* **1992**, *114* (14), 5530−5534.
(47) Jolly, P. I.; Zhou, S.; Thomson, D. W.; Garnier, J.; Parkinson, J. A.; Tuttle, T.; Murphy, J. A. Imidazole-derived carbenes and their elusive tetraazafulvalene dimers. *Chem. Sci.* **2012**, *3* (5), 1675−1679.
(48) Alder, R. W.; Blake, M. E.; Chaker, L.; Harvey, J. N.; Paolini, F.; Schütz, J. When and How Do Diaminocarbenes Dimerize? *Angew. Chem., Int. Ed.* **2004**, *43* (44), 5896−5911.
(49) Richter, C.; Schaepe, K.; Glorius, F.; Ravoo, B. J. Tailor-made N-heterocyclic carbenes for nanoparticle stabilization. *Chem. Commun.* **2014**, *50*, 3204−3207.
(50) Donakowski, M. D.; Godbe, J. M.; Sknepnek, R.; Knowles, K. E.; Olvera de la Cruz, M.; Weiss, E. A. A Quantitative Description of the Binding Equilibria of para-Substituted Aniline Ligands and CdSe Quantum Dots. *J. Phys. Chem. C* **2010**, *114* (51), 22526−22534.
(51) Moreels, I.; Martins, J. C.; Hens, Z. Ligand Adsorption/Desorption on Sterically Stabilized InP Colloidal Nanocrystals: Observation and Thermodynamic Analysis. *ChemPhysChem* **2006**, *7* (5), 1028−1031.
(52) Kohlmann, O.; Steinmetz, W. E.; Mao, X.-A.; Wuelfing, W. P.; Templeton, A. C.; Murray, R. W.; Johnson, C. S. NMR Diffusion, Relaxation, and Spectroscopic Studies of Water Soluble, Monolayer-Protected Gold Nanoclusters. *J. Phys. Chem. B* **2001**, *105* (37), 8801−8809.
(53) Khramov, D. M.; Lynch, V. M.; Bielawski, C. W. N-Heterocyclic Carbene-Transition Metal Complexes: Spectroscopic and Crystallographic Analyses of π-Back-bonding Interactions. *Organometallics* **2007**, *26* (24), 6042−6049.
(54) Swain, C. G.; Lupton, E. C. Field and resonance components of substituent effects. *J. Am. Chem. Soc.* **1968**, *90* (16), 4328−4337.
(55) Hansch, C.; Leo, A.; Taft, R. W. A survey of Hammett substituent constants and resonance and field parameters. *Chem. Rev.* **1991**, *91* (2), 165−195.
(56) Eastman, J. W. QUANTITATIVE SPECTROFLUORIMETRY-THE FLUORESCENCE QUANTUM YIELD OF QUININE SULFATE. *Photochem. Photobiol.* **1967**, *6* (1), 55−72.
(57) Polgar, A. M.; Weigend, F.; Zhang, A.; Stillman, M. J.; Corrigan, J. F. A N-Heterocyclic Carbene-Stabilized Coinage Metal-Chalcogenide Framework with Tunable Optical Properties. *J. Am. Chem. Soc.* **2017**, *139* (40), 14045−14048.

https://dx.doi.org/10.1021/jacs.9b13605
J. Am. Chem. Soc. 2020, 142, 2690−2696